

Facile Synthesis Protocol to the Preparation of Strontium Doped Copper Oxide for the Electrochemical Glucose Sensor

Munirathinam Elavarasan¹ and Thomas Chung-Kuang Yang^{1,2,*}

¹ Semiconductor Materials Lab, Department of Chemical Engineering and Biotechnology, National Taipei University of Technology, No.1, Section 3, Chung-Hsiao East Road, Taipei 106, Taiwan (R.O.C).

² Center of Precision Analysis and Material Research, National Taipei University of Technology, No.1, Section 3, Chung-Hsiao East Road, Taipei 106, Taiwan (R.O.C).

*E-mail: ckyang@mail.ntut.edu.tw

Received: 2 December 2018 / Accepted: 22 January 2019 / Published: 7 February 2019

This manuscript presents the facile synthesis protocol to prepare the strontium doped copper oxide (Sr-CuO) by the ligand exchange of copper nitrate ($\text{Cu}(\text{NO}_3)_2$) and strontium hydroxide ($\text{Sr}(\text{OH})_2$). The $\text{Sr}(\text{OH})_2$ is catalyzed the reaction to facilitate the CuO formation with Sr doping and also, it is furnished a well-defined leaf like morphology to Sr-CuO. The leaf like Sr-CuO nanoparticles are analyzed by the X-ray diffraction pattern (XRD), field emission scanning electron microscope (FESEM) and energy dispersive X-ray (EDX) studies. The Sr-CuO nanoparticles modified screen printed carbon electrode (SPCE) is used for the non-enzymatic glucose determination. The Sr-CuO/SPCE is effectively estimated the concentration of glucose with the acceptable analytical parameters. The estimated linear concentration range is 0.0001 to 11.5 mM and the lowest detection limit is 27 nM. Moreover, the Sr-CuO/SPCE glucose sensor exhibited good selectivity in the potential interfering compounds. These analytical performances of Sr-CuO/SPCE can greatly compared with the other CuO nanostructures.

Keywords: Leaf, ligand exchange, elemental mapping, copper oxyhydroxide, glucose mechanism.

1. INTRODUCTION

The past several decades revealed that the considerable improvement have progressed on the fast and reliable glucose sensor devices. Especially the electrochemical sensor devices, because of its real time monitoring are cost effective, rapid and easily accessible [1]. In general, the commercially available glucose sensor devices are based on the enzymatic reactions. Wherein, the glucose oxidase enzyme is utilized to oxidize the glucose into gluconolactone [2]. During the process, this enzyme also reacts with blood saturated oxygen molecule which produces the hydrogen peroxide (H_2O_2) [3]. Then, some other

enzymatic reactions are further used to determine the concentration of glucose with respect to the H_2O_2 concentration [4]. This enzymatic determination has some limitations because it may be affected by the oxygen, humidity, pH and temperature [5]. Therefore, the concept of non-enzymatic glucose sensor has been developed and many researches have already progressed. For instance, noble metals (Pd, Pt, Au) [6] and non-noble metals (mostly oxides of Ti, Mn, Fe, Co, Ni, Cu, Zn, W, Cd) [7] based sensors were reported. Among all, the Cu and Ni based compounds have exposed a good performance to the glucose determination [8], although, the oxides of Cu can perform even better than Ni. Therefore, varieties of Cu based nanostructures were fabricated for the non-enzymatic glucose sensors such as Cu-CuO nanowire [9] CuO nanocubes/graphene [10] CuO nanoplatelets [11] CuO nanorods-graphite [12] CuO nanospheres [13] Cu nanocluster-carbon nanotubes [14] CuO nanowires [15] CuO flowers-graphite [12] CuO biscuits/SPCE [16].

Besides morphology, several literatures were reported the bimetallic composites of CuO for the glucose determination. Recently, Wang group have reported palladium (IV)-doped CuO nanofibers for glucose sensors [17]. Interestingly, they have utilized the electrospinning technique to fabricate the Pd doped CuO nanofibers. Likewise, potassium-doped CuO nanoparticles (for lithium ion secondary battery [18]), zinc-doped CuO nanocrystals (for gas sensor [19]) and electron-doped CuO (for superconductors [20]) were reported. The aforesaid doped CuO compounds are utilized tedious synthesis protocol to prepare the materials of interest. But, we report the facile synthesis protocol to prepare the strontium (Sr) doped CuO by the ligand exchange method. The Sr is a good supportive element for the electro and photocatalytic applications thus Sr has selected as a dopant [21-24]. This Sr doping in CuO was confirmed by various physicochemical characterizations. Afterwards, Sr-CuO is coated on the SPCE and applied to the electrochemical studies.

2. EXPERIMENTAL SECTION

2.1 Materials

The copper nitrate trihydrate ($\text{Cu}(\text{NO}_3)_2 \cdot 3\text{H}_2\text{O}$), strontium hydroxide octahydrate ($\text{Sr}(\text{OH})_2 \cdot 8\text{H}_2\text{O}$), glucose, hydrogen peroxide and NaOH were purchased from Sigma-Aldrich, which are used as-received without any further purification. The screen printed carbon electrode (working area = 0.07 cm^2) was purchased from Zensor R&D Co., LTD, Taiwan.

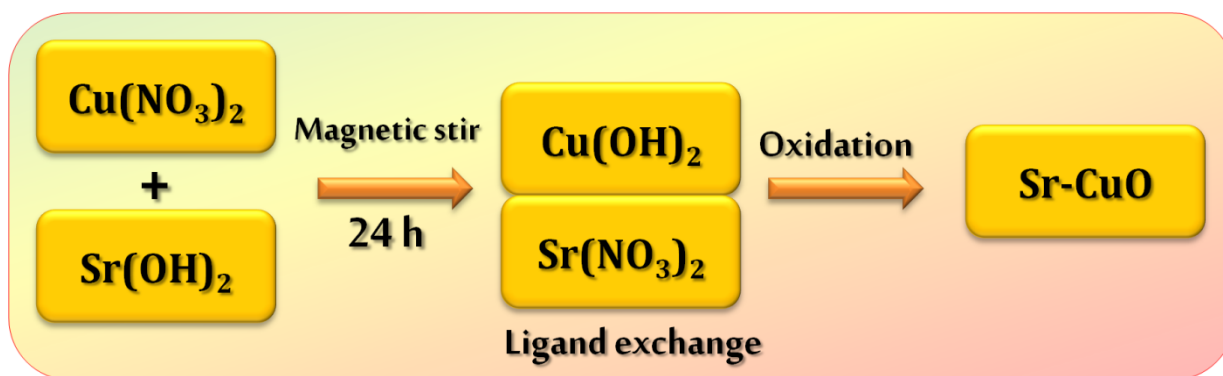
2.2 Methods

The doping of Sr in CuO lattice is scrutinized by XRD, XPERT-PRO (PANalytical B.V., The Netherlands) with $\text{CuK}\alpha$ radiation ($\lambda=1.5406 \text{ \AA}$) and also with FESEM, JEOL JSM-7610F attached with energy dispersive X-ray analyzer (EDX) from Oxford Instruments. The electrochemical studies are tested in CHI 1211c electrochemical analyzer (CH Instruments, USA). The electrochemical experimental setup was utilized three electrode system wherein the SPCE used as a working electrode,

saturated silver/silver chloride (Ag/AgCl) electrode as a reference electrode, the platinum wire as a counter electrode and 0.1 M NaOH is electrolyte.

2.3 Synthesis of Sr doped CuO

The Sr-CuO was prepared by the ligand exchange method, in that way, 15 mL of 50 mM $\text{Cu}(\text{NO}_3)_2$ was mixed with 15 mL of 50 mM $\text{Sr}(\text{OH})_2$. Suddenly, the solution color have changed to pale blue color and started to precipitate and then this mixer was kept in a magnetic stirrer and stirred for 24 hours. Herein, the $\text{Cu}(\text{NO}_3)_2$ was changed into $\text{Cu}(\text{OH})_2$ by hydroxyl ligand exchange. On the other hand, the $\text{Sr}(\text{OH})_2$ changed into $\text{Sr}(\text{NO}_3)_2$. Obviously, this is due to the ligand effect where copper have the high affinity when compared with strontium. During 24 hours stirring (27 °C), this suspension has a sequential color change from pale blue to dark brown. Afterwards, the precipitate was centrifuged and washed with water to remove the impurities. This compound was kept in a vacuum oven at 80 °C for 3 hours to completely evaporate the water molecules and also allowing to the formation of Sr-CuO. Then, the sample was grained well and used for the other characterizations. The overview of the synthesis protocol was portrayed in Scheme 1. For the comparative studies, the CuO was also synthesized by the same process wherein the sodium hydroxide was used instead of strontium hydroxide and also the mixture was heated for 80 °C to get the CuO.



Scheme 1. Schematic view of the overall synthesis process

2.4. Fabrication of modified SPCEs

The selection of SPCE as a substrate is a good choice for the sensor studies because it can be used as disposable electrode and also easy to fabricate [25]. Before electrode modification, the SPCEs are completely cleaned with the water and isopropyl alcohol mixer (1:1) to clean the surface. Meanwhile, the Sr-CuO and CuO samples were re-dispersed in double distilled (DD) water with the help of sonication. Afterwards, 7 μL of suspensions (either Sr-CuO or CuO) are tip coated on the SPCE and dried at 50 °C, after drying, the electrode was gently rinsed DD water to eliminate the freely bound Sr-CuO or CuO. These fabricated electrodes are further applied to the electrochemical determination of glucose.

3. RESULTS AND DISCUSSION

3.1. Characterizations of Sr-CuO

The simple ligand exchange method was utilized to prepare the Sr-CuO and we claim that it can be applicable for the doping process. However, the mechanism of the Sr doping in the CuO lattice is not clear. Though, we have tried to unveil the detailed mechanism of the Sr doping in CuO. Initially, the $\text{Cu}(\text{NO}_3)_2$ and $\text{Sr}(\text{OH})_2$ have the pH values of about 4.6 and 12.5 for the 50 mM concentrations. The pH value was suddenly dropped to 7.7 when both solutions mixed together, that means, the $\text{Cu}(\text{NO}_3)_2$ and $\text{Sr}(\text{OH})_2$ was exchanging their ligands and formed respective salts. Later, the $\text{Cu}(\text{OH})_2$ was slowly oxidized in air and converted to copper oxyhydroxide (CuOOH). Herein, the Sr ions are facilitated to the CuOOH formation because without Sr ion no color change has happened (that means in NaOH). Therefore, the $\text{Cu}(\text{OH})_2$ have a small amount of Sr ions in its lattice like $\text{Sr}_x\text{Cu}_{1-x}(\text{OH})_2$, this complex is later converted to Sr doped CuO. The experiment was repeated for 5 times to conclude the observed results which exhibited almost similar results for all experiments. To support this conjecture, the XRD and EDX analysis were used to confirm the Sr doping in CuO lattice.

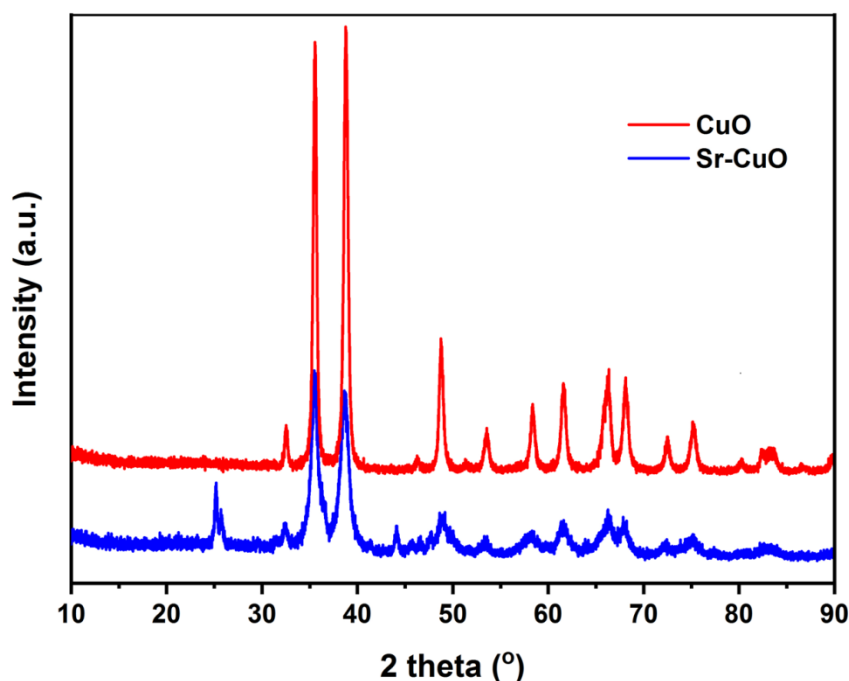


Figure 1. XRD patterns of CuO and Sr-CuO.

Figure. 1 shows the XRD patterns of CuO and Sr-CuO, the obtained peaks of both compounds are matched with the standard reference patterns (JCPDS-ICDD) of 05-0661 and 89-2529 respectively. The observed peaks at $2\theta = 32.52^\circ, 35.55^\circ, 38.73^\circ, 46.30^\circ, 48.76^\circ, 51.34^\circ, 53.41^\circ, 58.31^\circ, 61.57^\circ, 65.80^\circ, 66.22^\circ, 68.14^\circ, 72.41^\circ, 75.23^\circ, 80.18^\circ$ are corresponds to the planes (110), (-111), (111), (-112), (-202), (112), (020), (202), (-113), (022), (-311), (220), (311), (004), (-222), respectively, for the CuO [16] whereas Sr-CuO revealed the peaks at $32.42^\circ, 35.62^\circ, 38.44^\circ, 48.87^\circ, 53.41^\circ, 61.55^\circ, 66.26^\circ, 68.13^\circ, 72.24^\circ, 75.11^\circ$ for the respective planes.

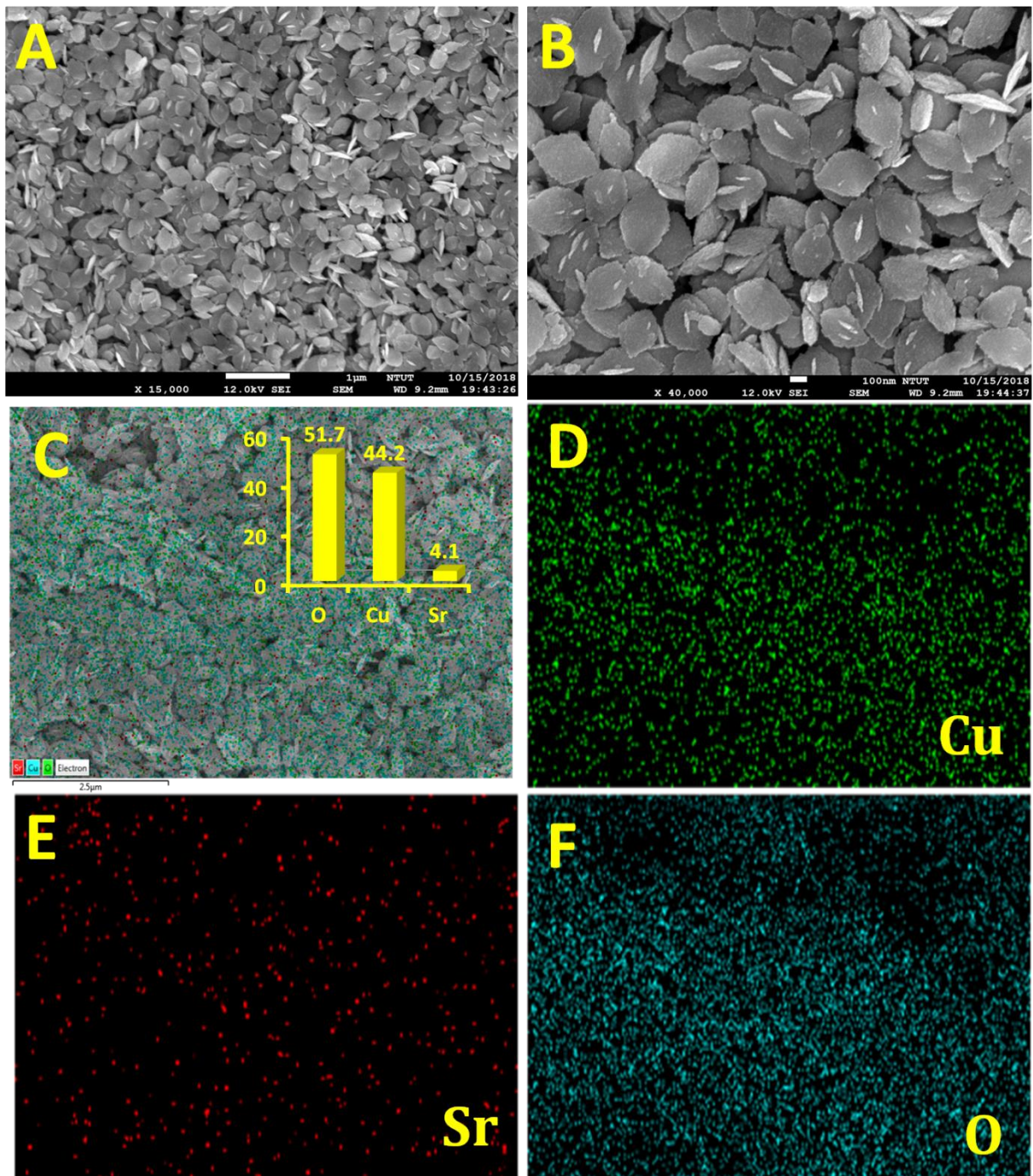


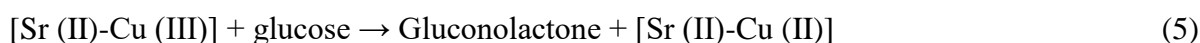
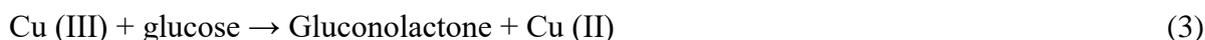
Figure 2. FESEM images of Sr-CuO nanoleaves in low magnification (A) and high magnification (B) view. (C) overlapping of overall elemental mapping and inset shows the atomic wt% of elements (D-F) individual elemental mapping of Cu, Sr and O.

This slight variation in the peak shift was inferred that slight structural quiver has happened in the Sr-CuO lattice. Considering crystal lattice, both compounds are having the same crystal system (monoclinic) and space group (C2/c) but the slight variation in its a, b, c values. Moreover, Sr-CuO exhibited some additional peaks at $2\theta = 25.14^\circ$, 25.75° , 29.66° , 44.09° , 45.63° and also have the peak broadness and high strain which confirmed that the Sr was doped in CuO lattice. Figure. 2 displays the low magnification (A) and high magnification (B) FESEM images of Sr-CuO, which looks like small

clusters of Sr-CuO are aggregated as leaf like morphology. These distinct leaves are having the uniform dimensions which possess the thickness about 10-30 nm and having the width about 100-200 nm. To further confirming the Sr doping, the EDX elemental mapping was taken for Sr-CuO. Figure. 2C displays the overlapped mapping of elemental distribution which showed the overall elemental composition is O=51.7 %, Cu=44.2 % and Sr=4.1 % (for the average mapping results of 50 μm^2). Moreover, Figure. 2D to 2F showing the individual distribution of Cu, Sr and O. These EDX mappings is evinced that the Sr is replacing the Cu in CuO lattice, hence, this analysis confirmed that Sr is doped in CuO lattice.

3.2. Electrochemical oxidation of glucose at Sr-CuO/SPCE

The electrochemical oxidation of glucose at the CuO/SPCE and Sr-CuO/SPCE was examined by CV in 0.1 M NaOH containing 1 mM glucose at the scan rate of 50 $\text{mV}\cdot\text{s}^{-1}$. Prior to that, the glucose oxidation was analyzed for bare SPCE, it revealed no response for the glucose and also exhibited very low background signal (data not shown due to the clumsy depiction in figure) which confirmed that there is no substrate effect was influenced by SPCE. In contrast, CuO/SPCE showed the response signal for glucose oxidation which starting from +0.37 V and peaks at +0.55 V (Figure. 3A). This value is similar to the most of copper-based glucose sensors as reported in literatures [8,16]. Herein, the redox reaction of Cu (II) to Cu (III) in the CuO/SPCE facilitates the glucose oxidation. However, there is no redox couple visible in the CV curve (absence of glucose) of CuO/SPCE thus it may be considered as intrinsic redox reactions of CuO. On the other hand, Sr-CuO/SPCE revealed the high background signal for those redox couple centered at +0.38 V and also it shows an additional reduction peak at +0.58 V which attributed to the reduction of strontium hydroxide in Sr-CuO lattice. Mostly, the $\text{Cu}^{2+/3+}$ redox couple is responsible for the glucose oxidation however the Sr ions are helped to enhance the activity by contributing its orbital with the CuO. Therefore, this study confirmed the Sr-CuO/SPCE has a good electrochemical activity when compared to CuO/SPCE. The equations 1-3 shows the general glucose oxidation mechanism at copper-based compounds, however the mechanism is unknown for the Sr-CuO, though, we have tried to summarize that in equation 4 and 5. Initially, the Cu (II) undergoes electrooxidation to Cu (III) and this Cu (III) is oxidized the glucose into gluconolactone and then it regains its electrons back. Hence, the glucose oxidation on CuO follows the CE mechanism, the same way Sr-CuO also oxidized the glucose. Herein, the Sr ions are only support the CuO to proceeds the reaction faster.



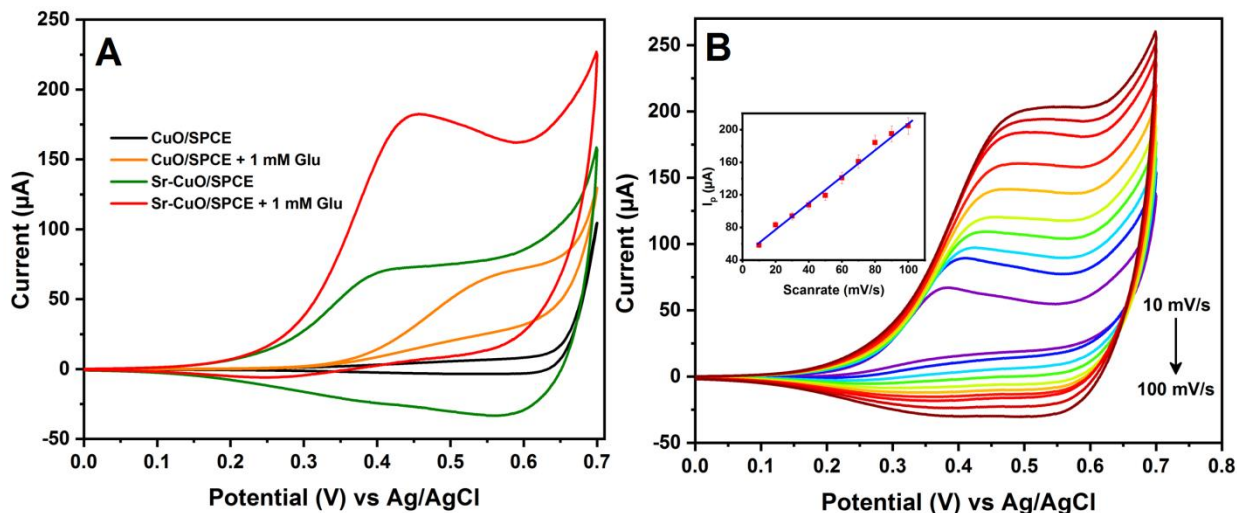


Figure 3. CV responses of CuO/SPCE and Sr-CuO/SPCE recorded in 0.1 M NaOH in the presence and absence of 1 mM (A). The various scan rate analysis of glucose oxidation at Sr-CuO/SPCE for the scan rates ranging from 10 to 100 mV/s (B) and inset showing the linear plot for the peak current vs. scan rate.

To evaluate the electrode kinetics, the glucose oxidation was performed on Sr-CuO/SPCE for various scan rates. Figure. 3B displays the scan rate analysis of glucose oxidation at Sr-CuO/SPCE for the scan rates ranging from 10 to 100 $\text{mV}\cdot\text{s}^{-1}$. The oxidation peak current was successively increased when the scan rates were increased then it was plotted against the scan rate as displayed in Figure. 3B (inset). The data points are following the linearity which suggested that the glucose oxidation at Sr-CuO/SPCE was adsorption controlled [26]. In most cases, the glucose was initially adsorbed on the surface of the substrate because of many hydroxyl functional groups. Later, it will detach the surface when it converted to gluconolactone.

3.3. Determination of glucose

The preliminary studies of glucose oxidation at the Sr-CuO/SPCE suggested that it can be applicable for the real time glucose monitoring sensor electrode because of low cost and disposable electrode. Thereby, the glucose determination on Sr-CuO was evaluated by the amperometry technique. From the CV studies, we already optimized the conditions of glucose oxidation thus we directly fixed +0.45 V as an oxidation potential. The amperometric determination of glucose was shown in Figure. 4A. Herein, the glucose was successively added into the continuously stirred 0.1 M NaOH by different concentrations ranging from 0.0001 to 14.5 mM. The first addition was started at 300 s where it gave the sharp peak for the 100 nM glucose within 0.8 s. This is the fastest response for the glucose oxidation on Sr-CuO. After the response current, it achieved the steady state current in less than 1 s. Then, the time of successive addition was maintained by 50 s intervals.

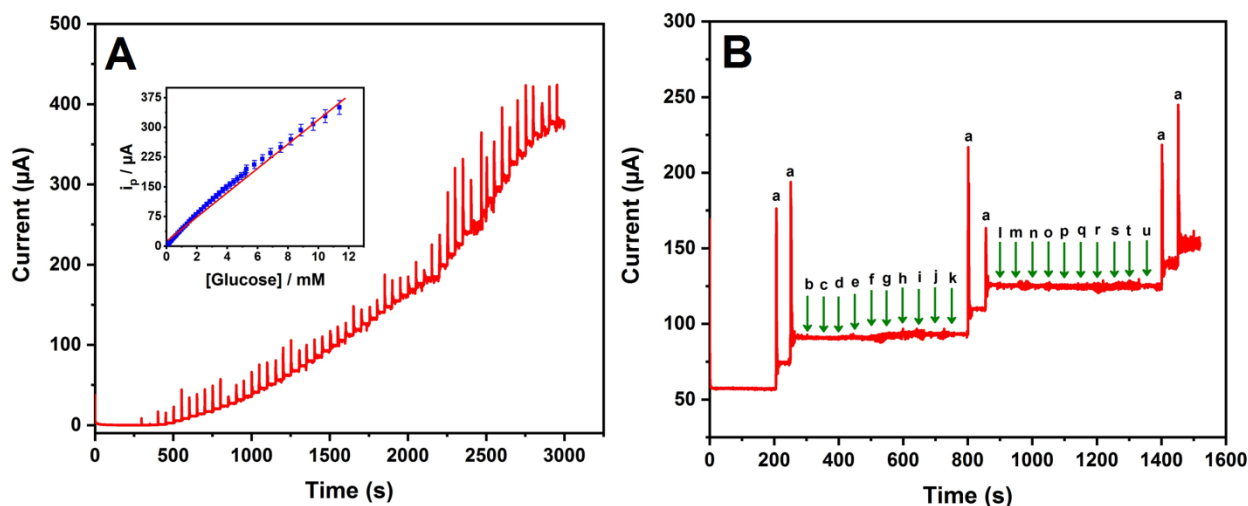


Figure 4. The amperometric (it) determination of glucose on Sr-CuO/SPCE with the consecutive additions of glucose in the range of 0.0001 to 14.5 mM (B) and inset shows the calibration of glucose determination. (B) the selectivity analysis of glucose determination performed in 0.1 M NaOH in the presence of 0.5 mM glucose (a) sucrose (b), fructose (c), galactose (d), DA (e) AA (f) H₂O₂ (g) UA (h), H₂O₂ (i), Ach (j), NADH (k) and NO₂⁻ (l), tryptophan (m), serotonin (n), Mg²⁺ (o), Cu²⁺ (p), Fe²⁺ (q), Zn²⁺ (r), Fe³⁺ (s), Co²⁺ (t), Ni²⁺ (u).

As shown in Figure. 4A, the oxidation current was consecutively increased while successively increased the concentration of the glucose. Then the oxidation current was plotted against the concentration of the glucose and shown in Figure. 4A inset. This plot detailed the information about the sensitivity, linear range and lowest detection limit (LOD). The experiment was repeated for 5 times and the data points were processed with the statistical analysis [31]. From the obtained data, Sr-CuO/SPCE revealed a wide linear range and LOD about 0.0001 to 11.5 mM and 27 nm, respectively. Mostly, the glucose level in blood varies from 3 to 8 mM hence the obtained analytical parameters are appropriate for the real time applications. These analytical parameters were compared with the previously reported CuO based glucose sensors and given in Table 1.

Table 1. Comparison on the analytical performances of Sr-CuO nano-leaves/SPCE with other nanostructured CuOs.

Electrode materials	Potential (V)	Linear range (up to, mM)	Detection limit (μM)	Ref
Cu-CuO nanowire	0.3	12	500	[9]
CuO flowers-graphite	0.60	–	4.0	[12]
CuO nanorods-graphite	0.60	8.0	4.0	[12]
CuO nanospheres	0.60	2.6	1.0	[13]
CuO nanoplatelets	0.55	0.8	0.5	[11]
Cu nanocluster-CNTs	0.65	3.5	0.21	[14]
CuO biscuits/SPCE	0.5	4.03	0.1	[16]
CuO nanowires	0.33	2.0	0.049	[15]
Pd doped CuO	0.32	2.5	0.019	[17]
CuO	0.5	4.0	0.5	[32]
Sr-CuO/SPCE	0.45	11.54	0.027	This work

3.4. Interference study

Selectivity is an important parameter for the sensor devices thereby Sr-CuO/SPCE was subjected to the selectivity test. Herein, the glucose is going to determine in the presence of some other substances which usually interfere with the glucose signal. In general, the glucose is co-exists with some biological compounds (ascorbic acid (AA), uric acid (UA) and dopamine (DA)) and also other carbohydrate derivatives in the blood [27]. But, most of the other carbohydrate derivatives are electrochemically less active than glucose. In addition, some other metabolized reagents like hydrogen peroxide (H_2O_2), acetylcholine (Ach) and nicotinamide adenine dinucleotide (NADH) also interferes with glucose oxidation. Therefore, the glucose determination on Sr-CuO/SPCE is examined in 0.1 M NaOH containing 0.5 mM glucose in the presence of sucrose (b), fructose (c), galactose (d), DA (e) AA (f) H_2O_2 (g) UA (h), H_2O_2 (i), Ach (j), NADH (k) and NO_2^- (l), tryptophan (m), serotonin (n), Mg^{2+} (o), Cu^{2+} (p), Fe^{2+} (q), Zn^{2+} (r), Fe^{3+} (s), Co^{2+} (t), Ni^{2+} (u). The biological compounds are taken by 20 times lower than glucose concentrations and metal ions are taken by 10 lower than glucose concentrations. Herein, the concentrations of interfering compounds are taken with respect to the physiological level of glucose concentration (probably, 3–8 mM) [28]. Fig. 4D shows the amperometric response of glucose oxidation on Sr-CuO/SPCE in the presence of interfering compounds. All the other experimental parameters were followed as given in section 3.3. The sharp signal (a) is represents the glucose oxidation whereas no noticeable responses were appeared for the consecutive additions of other interfering compounds. However, some of noise signal were observed in the steady state current response which may due to the metal hydroxides formation because the metal ions were precipitated in the NaOH [29]. Moreover, the H_2O_2 also makes some noise perturbation due to surface adsorbed oxidative reaction of H_2O_2 [30]. Anyhow, the response signal of interfering compounds doesn't affect the glucose response signal therefore this Sr-CuO/SPCE can be used as a disposable electrode for the glucose determination.

3.5 Real sample analysis

The practicability of Sr-CuO/SPCE glucose sensor investigated in the determination of glucose in blood samples. According to the literatures, the approximate glucose level in blood samples are 4.95 mM for non-diabetic patients [33,34]. Our reported material exhibited the acceptable detection range to determine the glucose in blood samples. The blood samples are diluted with DI water for the appropriate concentrations and directly used for the glucose determination. The similar experimental procedure was followed as discussed in *section 3.3*. The Sr-CuO/SPCE glucose sensor electrode has shown the good recoveries for the blood samples (Table 2). Moreover, the obtained results were compared with commercial glucose sensor device, which shows minimal error with Sr-CuO/SPCE. Therefore, Sr-CuO/SPCE could be applicable for the real time sensing of glucose.

Table 2. The recoveries for the determination of glucose in blood samples.

Real sample	Add (μM)	Found ^a (μM)	Recovery (%)	RSD ^b (%)
Sample 1	-	10.2	-	-
	10	20.0	99.0	3.2
Sample 2	-	13.6	-	-
	10	23.4	99.1	2.9
Sample 3	-	17.6	-	-
	10	27.3	98.9	3.1

^aStandard deviation method and ^bRelative standard deviation with three repetitive measurements.

4. CONCLUSIONS

In summary, the Sr doped CuO nanoparticles was successfully prepared and characterized by XRD and EDX analysis. Interestingly, the Sr(OH)₂ is efficiently catalyzed the reaction and furnished the Sr-CuO as leaf-like shape. The Sr doping was critically scrutinized by XRD and EDX analysis which results that approximately 4.1 % of Sr was doped in CuO lattice, however, the lattice parameters are not changed significantly. Then, Sr-CuO/SPCE is tested for the non-enzymatic glucose determination which exhibited better analytical performances than CuO/SPCE. The observed linear range, limit of detection and oxidation potential was compared with previously reported CuO based sensors that shows Sr-CuO/SPCE have better activity. Moreover, it is selectively determined the glucose in the presence of important interfering compounds. Therefore, Sr-CuO/SPCE is suitable for the disposable glucose sensors which can determine glucose in the concentration range of 0.0001 mM to 11.5 mM.

ACKNOWLEDGEMENT

This project was supported by the Ministry of Science and Technology of Taiwan (Republic of China). Authors also acknowledge the Center of Precision Analysis and Material Research, National Taipei University of Technology for providing the all necessary Instrument facilities.

References

1. J. Wang, *Chem. Rev.*, 108 (2008) 821.
2. N. Karikalan, M. Velmurugan, S.M. Chen and C. Karuppiyah. *ACS Appl. Mater. Interfaces*, 8 (2016) 22545.
3. S. Ci, T. Huang, Z. Wen, S. Cui, S. Mao, D. A. Steeber and J. Chen, *Biosens. Bioelectron.*, 54 (2014) 250.
4. G. G. Guilbault and G. J. Lubrano, *Anal. Chim. Acta*, 64 (1973) 439.
5. Z. G. Zhu, L. Garcia-Gancedo, A. J. Flewitt, H. Q. Xie, F. Moussy and W. I. Milne, *Sensors*, 12 (2012) 5996.
6. G. Wang, X. He, L. Wang, A. Gu, Y. Huang, B. Fang, B. Geng and X. Zhang. *Microchim. Acta*, 180 (2013) 161.
7. P. Si, Y. Huang, T. Wang and J. Ma, *RSC Adv.*, 3 (2013) 3487.

8. N. Karikalan, R. Karthik, S.M. Chen, C. Karuppiah, and A. Elangovan, *Sci. Rep.*, 7 (2017) 2494.
9. G.F. Wang, Y. Wei, W. Zhang, X.J. Zhang, B. Fang and L. Wang, *Microchim. Acta*, 168 (2010) 87.
10. L.Q. Luo, L.M. Zhu and Z.X. Wang. *Bioelectrochemistry*, 88 (2012) 156.
11. J. Wang and W.D. Zhang, *Electrochim. Acta*, 56 (2011) 7510.
12. X. Wang, C.G. Hu, H. Liu, G.J. Du, X.S. He and Y. Xi, *Sens. Actuators B Chem.*, 144 (2009) 220.
13. E. Reitz, W.Z. Jia, M. Gentile, Y. Wang and Y. Lei, *Electroanal.*, 20 (2008) 2282.
14. X.H. Kang, Z.B. Mai, X.Y. Zou, P.X. Cai and J.Y. Mo, *Anal. Biochem.*, 363 (2007) 143.
15. Z.J. Zhuang, X.D. Su, H.Y. Yuan, D. Xiao and M.M.F. Choi, *Analyst*, 133 (2008) 126-132.
16. M. Velmurugan, N. Karikalan and S.M. Chen, *J. Colloid Interface Sci.*, 493 (2017) 349.
17. W. Wang, Z. Li, W. Zheng, J. Yang, H. Zhang and C. Wang, *Electrochem. Commun.*, 11 (2009) 1811.
18. T.V. Thi, A.K. Rai, J. Gim and J. Kim, *Appl. Surf. Sci.*, 305 (2014) 617.
19. V. Cretu, V. Postica, A.K. Mishra, M. Hoppe, I. Tiginyanu, Y.K. Mishra, L. Chow, N.H. De Leeuw, R. Adelung and O. Lupan, *J. Mater. Chem. A*, 4 (2016) 6527.
20. J. M. Tranquada, S. M. Heald, A. R. Moodenbaugh, G. Liang and M. Croft. *Nature* 337 (1989) 720.
21. R. Karthik, N. Karikalan, S.M. Chen, J.V. Kumar, C. Karuppiah and V. Muthuraj, *J. Catal.*, 352 (2017) 606.
22. C. Niu and C.M. Lieber, *J. Am. Chem. Soc.*, 114 (1992) 3570.
23. S. Brochen, L. Bergerot, W. Favre, J. Resende, C. Jiménez, J.L. Deschanvres and V. Consonni, *J. Phys. Chem. C*, 120 (2016) 17261.
24. L. Bergerot, C. Jiménez, O. Chaix-Pluchery, L. Rapenne and J.L. Deschanvres, *physica status solidi (a)* 212 (2015) 1735.
25. N. Karikalan, R. Karthik, S.M. Chen, M. Velmurugan and C. Karuppiah, *J. Colloid Interface Sci.*, 483(2016) 109.
26. J. Luo, S. Jiang, H. Zhang, J. Jiang and X. Liu. *Anal. Chim. Acta*, 709 (2012) 47.
27. Y. H. Ni, L. N. Jin, L. Zhang and J. M. Hong, *J. Mater. Chem.*, 20 (2010) 6430.
28. R. M. Abdel Hameed, *Biosens. Bioelectron.*, 47 (2013) 248.
29. M. Velmurugan, N. Karikalan, S.M. Chen and C. Karuppiah, *Microchim. Acta*, 183 (2016) 2713.
30. R. Karthik, N. Karikalan and S.M. Chen, *Carbohydr. Polym.*, 164 (2017) 102.
31. S. Kubendhiran, N. Karikalan, S.M. Chen, P. Sundaresan, and R. Karthik, *J. Catal.*, 367 (2018) 252.
32. X. Ma, Q. Zhao, H. Wang, and S. Ji, *Int. J. Electrochem. Sci*, 12 (2017) 8217.
33. Z. Nie, C. A Nijhuis, J. Gong, X. Chen, A. Kumachev, A. W. Martinez, M. Narovlyansky, G. M. Whitesides, *Lab Chip*. 10 (2010) 477.
34. R. P. Agrawal, N. Sharma, M. S. Rathor, V. B Gupta, S. Jain, V. Agarwal, S. Goyal, *J. Diabetes Metab.* 4 (2013) 266.